

Plastics–Fertilizer Homology: Solid-Phase Molecular Assembly Enables Natural Closed-Ring Cycle of Biomass-like Plastics

Jinwan Qi,[#] Hongxin Zhao,[#] Hongjun Jin,[#] Shuitao Gao, Jianbin Huang, Xinxian Ma,^{*} and Yun Yan^{*}Cite This: *ACS Materials Lett.* 2025, 7, 1646–1653

Read Online

ACCESS |



Metrics & More

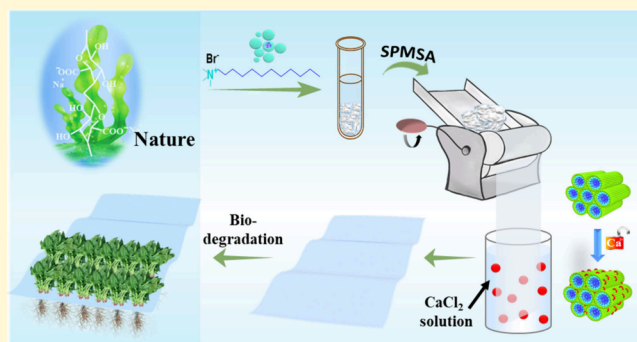


Article Recommendations



Supporting Information

ABSTRACT: Biomasses have undergone natural closed-ring cycles for billions of years, including biodegradation, soil fertilization, and transformation to new biomass through neutralizing plants. If a bioplastic is made biomass-like, its natural closed-ring cycle would be very promising in tackling the white pollution and microplastics problems associated with petroleum plastics. Herein we report a proof-of-concept strategy employing plastics–fertilizer homology toward this goal. Biomass-like supramolecular plastics were fabricated through solid-phase molecular self-assembly of alginate and alkylammonium surfactants, followed by calcium coordination. The resultant plastics display satisfactory dry and wet mechanical strength, comparable to that of conventional petroleum plastics, while being fully biodegradable. The biodegradation products were able to increase pak choi's wet/dry weights by 40% and 12%, respectively, promoting both soil fertility and water retention. This natural closed-ring cycle is very similar to real biomass processes, verifying the plastics–fertilizer homology as a promising solution to white pollution and microplastics crises.



White pollution from plastics has triggered global concern about the environment.^{1–5} Biodegradable plastics had been proposed as efficient alternatives to tackle this problem.^{6–13} However, so far most biodegradable plastics have a risk of incomplete biodegradation, which may lead to an even more serious ecological problem with microplastics. To date, microplastics have been reported to delay plant growth, trigger gene mutation, and potentially be cancerous.^{14–16} Under this background, the development of biodegradable plastics seems illusive. Instead, researchers' efforts are switching to closed-ring cycles^{17–21} and catalyzed degradation^{22–24} of plastics.

As petroleum products, plastics are long-chain polymers with low polarity, which makes it very difficult for them to adsorb water and interact with microorganisms, resulting in their accumulation in the environment.^{25,26} In contrast, the natural polymeric biomass, including proteins, polysaccharides, polyphenols, which are all polar, can be completely degraded by microorganisms into water, carbon dioxide, and other nutrient materials that are advantageous to soil.^{27–29} The biodegradation of biomass would promote soil fertility, which would enhance the growth of plants, achieving a natural closed-ring cycle. With thousands of years of such natural closed-ring cycles, Nature is

able to develop sustainably. We therefore propose that if a plastics–fertilizer homology can be achieved, the natural closed-ring cycle of plastics would benefit soil fertility and plant growth, so that plastic pollution could be removed in a sustainable way.

To this end, herein we report a case of supramolecular plastics made from a biopolysaccharide and a small amphiphilic molecule. The biopolysaccharide sodium alginate (SA) is a well-known biostimulus to promote plant root and leaf growth in agriculture.^{30,31} In order to make it into plastics, SA was employed for molecular self-assembly with the cationic surfactant dodecyl trimethylammonium bromide (DTAB) through mechanical pressing of their precipitates, which was termed as solid-phase molecular self-assembly (SPMSA).^{32–36} Compared with the conventional strategy of casting films, which requires slow evaporation of the solvent, the mechanical pressure in SPMSA facilitates quick film formation with much

Received: January 2, 2025

Revised: March 26, 2025

Accepted: March 26, 2025

Scheme 1. Fabrication of Biomass-like SA-DTAB-Ca Supramolecular Plastics and Their Natural Closed-Ring Cycle Enabled by Promoting Plant Growth

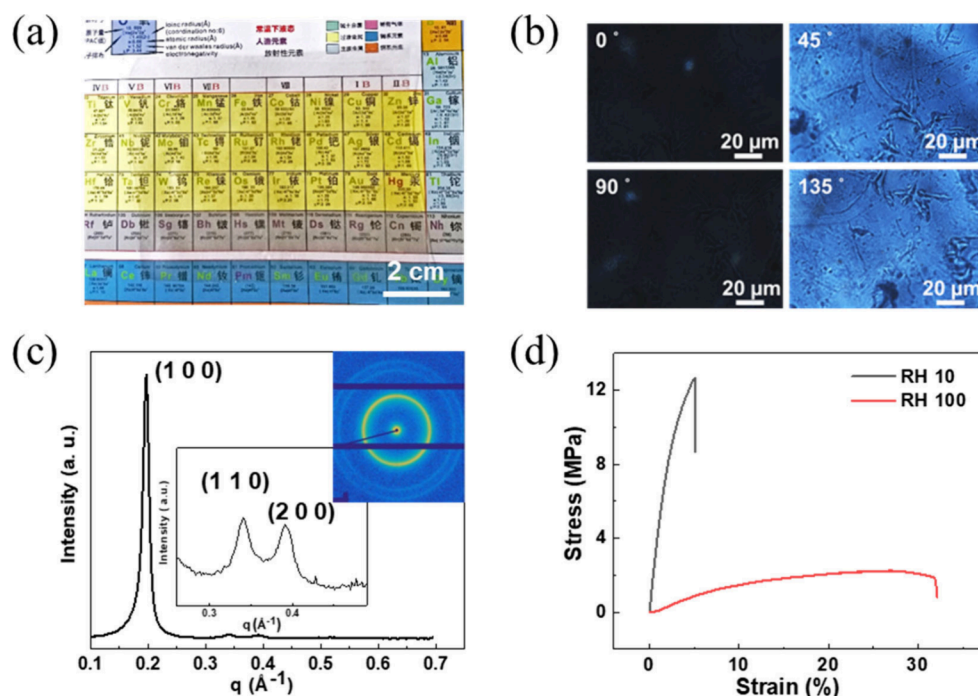
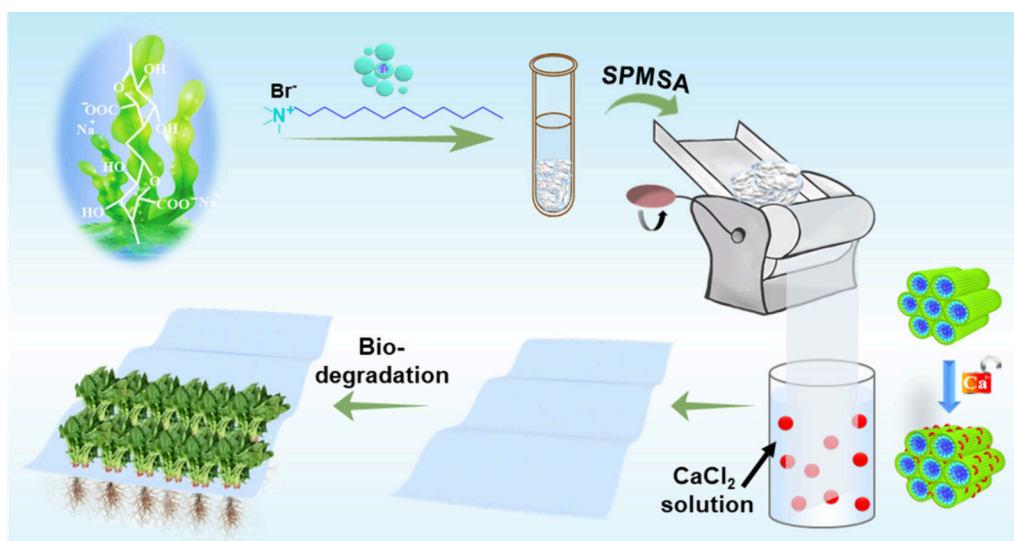


Figure 1. Structure and properties of the SA-DTAB film. (a) Optical photograph of the prepared SA-DTAB film. (b) Polarized optical microscopy images of the SA-DTAB film at different angles. (c) 2D-MAXS patterns and a one-dimensional integration of the SA-DTAB film. (d) Strain–stress curves of the SA-DTAB film under different humidity environments. RH 10 and RH 100 refer to the environment's relative humidity of 10% and 100%, respectively.

better molecular arrangement, which has been well-established in our previous work. Considering that the charged polar groups in SPMSA would absorb water in high humidity and lose water in low humidity, causing poor mechanical strength in water and dry brittleness of the resultant supramolecular plastics, respectively, we further immersed the SA-DTAB film into solutions containing Ca^{2+} to cross-link the SA chains via coordination interaction. Surprisingly, this caused replacement of 90% of the DTAB with Ca^{2+} , and the resultant supramolecular plastics became mechanically robust in water but remained flexible even in dry environments. In this way, the final plastic displays ideal wet and dry resistance, similar to that of

conventional polyethylene and polypropylene plastics, but can be biodegraded in a natural environment within 90 days and can promote the growth of plants, indicating the promising possibility of plastics–fertilizer homology.

Scheme 1 demonstrates the process of SPMSA of SA and DTAB. Their aqueous solution was mixed at a charge-balancing ratio to get an amorphous precipitate. Then the precipitate was collected and subjected to a household noodle machine (**Supplementary Figure 1a**) to generate a birefringent transparent supramolecular film (**Figure 1a,b** and **Supplementary Figure 1b**). The thickness of the resulting SA-DTAB film can be easily adjusted between 10 and 1000 μm by controlling the

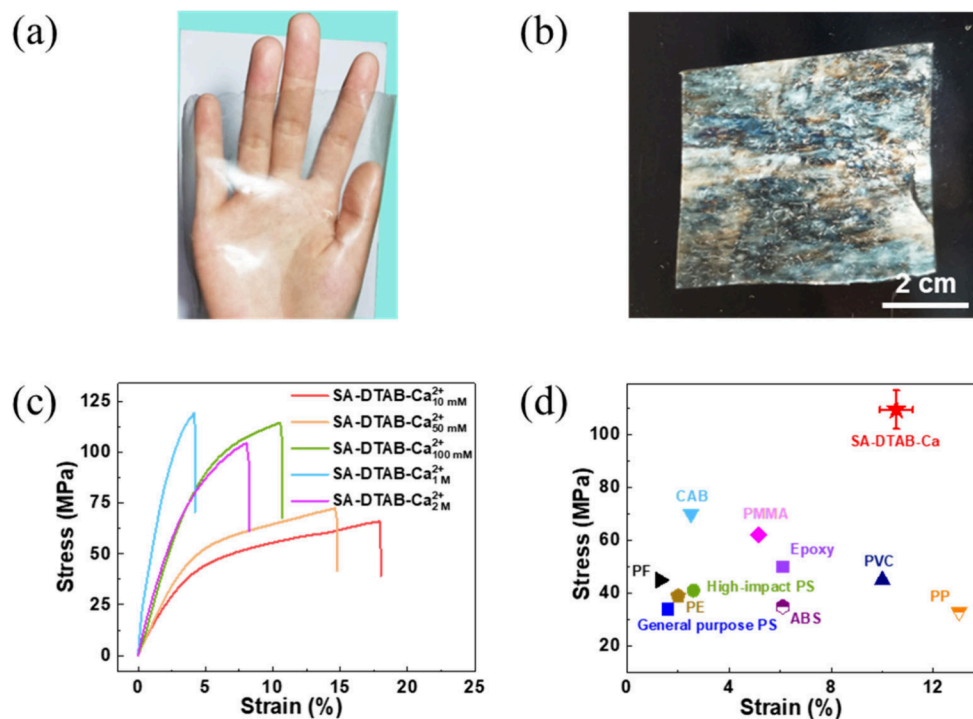


Figure 2. Structure and mechanical properties of the SA-DTAB-Ca film. (a) Optical photograph of the prepared SA-DTAB-Ca²⁺_{100 mM} plastics. (b) Birefringence of the SA-DTAB-Ca²⁺_{100 mM} film observed between two vertically aligned polarizers. (c) Tensile stress–strain curves of the SA-DTAB films immersed in CaCl₂ solutions of different concentrations for 5 h at 25% RH and room temperature. (d) Comparison of the tensile strength of the dry SA-DTAB-Ca²⁺_{100 mM} film with that of conventional petroleum plastics.

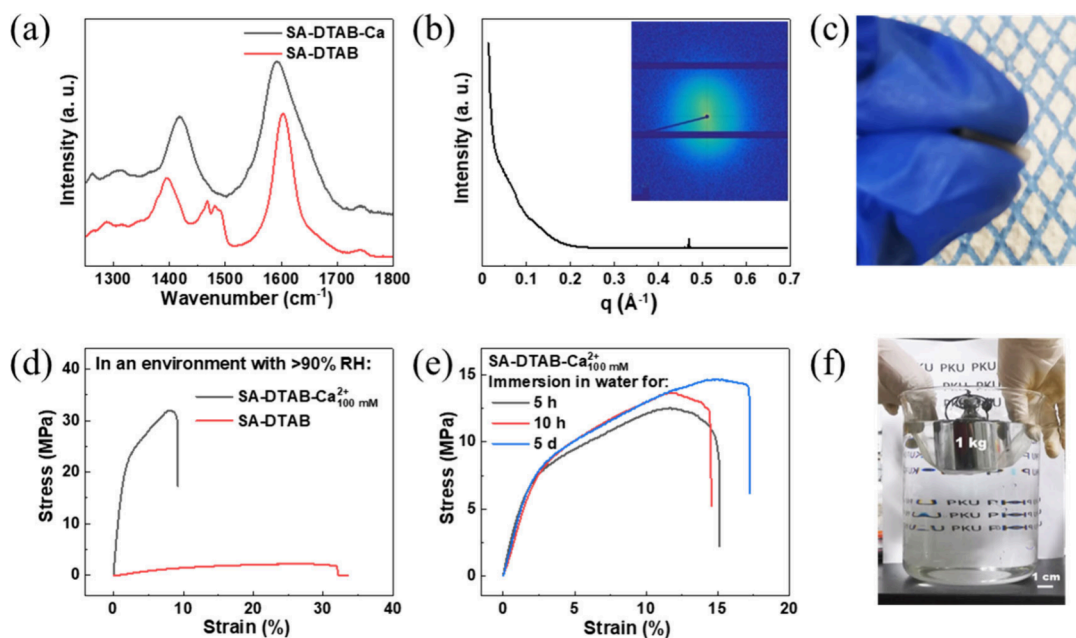


Figure 3. Spectra and diffraction properties of the SA-DTAB-Ca²⁺_{100 mM} film and its mechanical strength in a humid environment and in water. (a) ATR-IR spectra of the SA-DTAB and SA-DTAB-Ca films. (b) 2D-MAXS patterns and a one-dimensional integration curve of the SA-DTAB-Ca film. (c) Flexibility of the SA-DTAB-Ca film after drying at 80 °C overnight. (d) Stress–strain curves of SA-DTAB and SA-DTAB-Ca²⁺_{100 mM} plastics after being exposed to an environment of >90% RH at 25 °C for 7 d. (e) Stress–strain curves of SA-DTAB and SA-DTAB-Ca²⁺_{100 mM} plastics after being immersed in water for different periods. (f) Photograph of the film soaked in water, loaded with a 1 kg weight.

spacing between the noodle pressing rolls. XRD measurements reveal that the DTAB molecules formed bilayers (Figure 1c), which are characterized by a distance of 3.36 nm, namely, about 2-fold the chain length of DTAB in the XRD patterns (Supplementary Figure 2). Elemental analysis reveals that the

molar ratio of COO[−] and DTA⁺ units is about 1:1, indicating the DTA⁺ bilayers are electrostatically connected by the SA chains (Supplementary Table 1). This primary fresh SA-DTAB film, with a mechanical strength less than 12 MPa, becomes fragile at relative humidity (RH) lower than 30%, and the mechanical

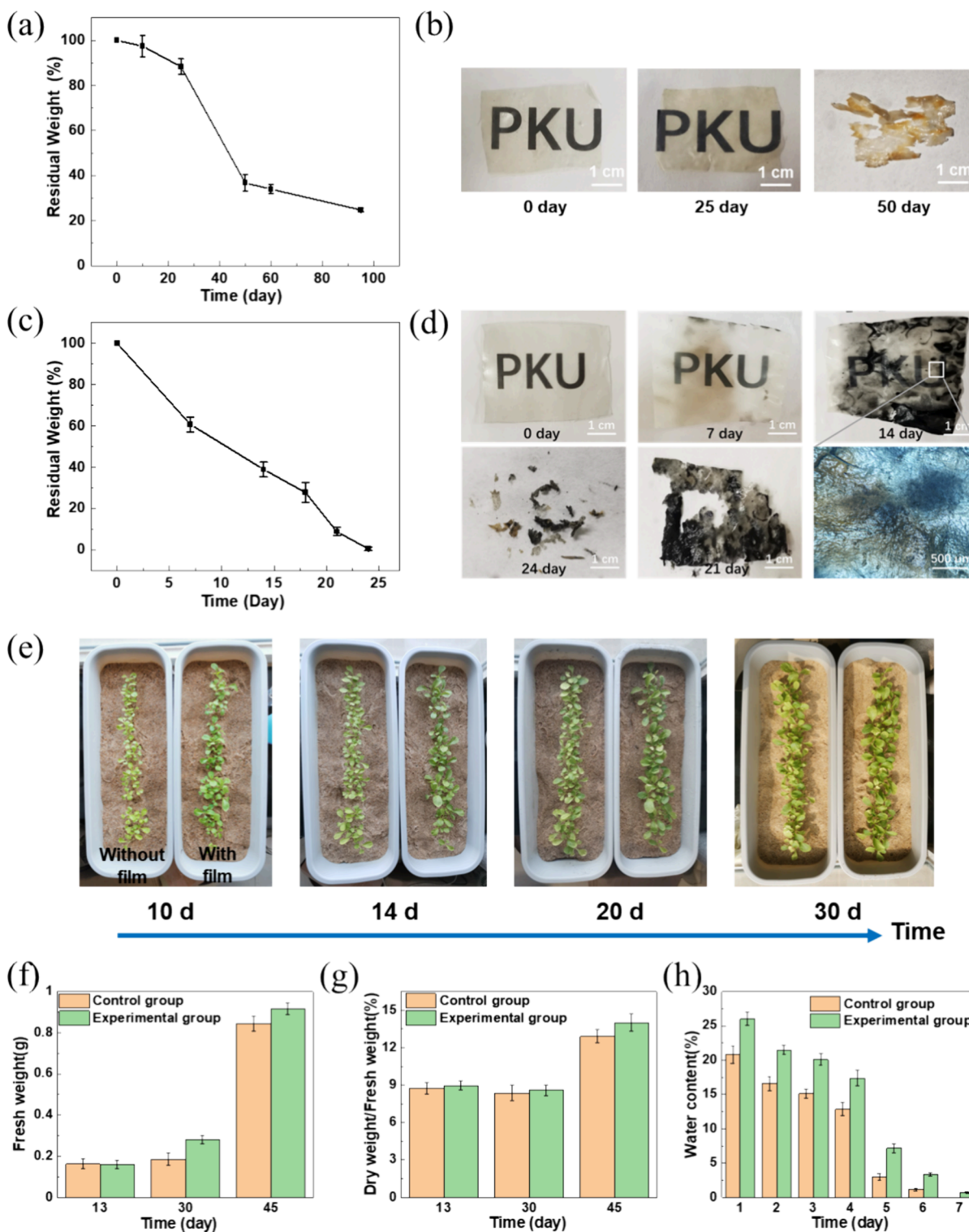


Figure 4. Natural biodegradation of the plastics and the impact on plant growth and soil fertility. (a) Residual weight of the plastics as a function of time under natural soil. (b) Digital images of the intact plastic after being buried under natural soil for 0, 25, and 50 days. (c) Residual weight of the plastics as a function of time under soil consisting of potting media and composting microorganisms in a weight ratio of 4:1. (d) Digital images of the intact plastic and of the plastics after being buried under soil for 0, 7, 14, 21, and 24 days in potting media. (e) Digital images of the growth of pak choi in the sand without (control group) and with buried film (experimental group; plastic film of same size as the vessel was buried 5 cm under the sand surface) for 10, 14, 20, and 30 days. Fresh weight (f) and dry mass (dry weight/fresh weight, g) of pak choi grown in the sand without (control group) and with buried film (experimental group) for 13, 30, and 45 days. (h) Time-dependent water content of the sand without (control group) and with buried film (experimental group).

strength decreases to 1.8 MPa at 100% RH (Figure 1d), which is not useful for practical applications.

In order to improve the dry and wet resistance of the primary SA-DTAB film, it was immersed in an aqueous solution of CaCl_2

to cross-link the alginate chain through Ca^{2+} coordination with the COO^- groups, which not only decreases the water-binding ability of COO^- but also reduces the fraction of moisture-absorbing DTA^+ cations in the film. Figure 2a shows that, after this treatment, the film remained transparent but with different birefringence (Figure 2b). Mechanical tests revealed that the tensile strength reached its maximum upon immersion of the film in 100 mM CaCl_2 for 5 h (Figure 2c and Supplementary Figure 3). Further increasing the concentration of CaCl_2 did not promote the mechanical strength noticeably but did reduce the strain and decrease the film's flexibility (Supplementary Figure 4). It is noticed that the tensile strength of the film obtained in 100 mM CaCl_2 was about 120 MPa, which is much higher than that of most conventional plastics, as illustrated in Figure 2d.

Elemental analysis studies revealed that, after treatment with 100 mM Ca^{2+} , the film was composed of $\text{SA-DTA}^+_{0.3}\text{-Ca}^{2+}_{0.3}$ (Supplementary Table 1), indicating that 70% of the DTA^+ cations were replaced by Ca^{2+} . In line with this, the COO^- symmetric vibrational bands at 1420 cm^{-1} in the ATR-IR spectra (Figure 3a and Supplementary Figure 5) have doubled, indicative of the coordination between Ca^{2+} and the COO^- group of SA (Supplementary Figure 6). Meanwhile, the bilayer diffraction was blurred in XRD (Figure 3b and Supplementary Figure 7), which corresponds to the vanishing of densely packed DTA^+ bilayers. It is noteworthy that the $\text{SA-DTA}^+_{0.3}\text{-Ca}^{2+}_{0.3}$ plastic displays excellent wet and dry resistance. The film remains flexible even after being heated to $80\text{ }^\circ\text{C}$ overnight to dry it sufficiently (Figure 3c). On the other hand, it still possesses a high mechanical strength of 32 MPa after incubation at a relatively high humidity of 90% for 5 days (Figure 3d). This mechanical strength is comparable to that of most petroleum plastics for daily use (Figure 2d and Supplementary Figure 8).^{37,38} Figure 3e shows that the $10\text{ cm} \times 10\text{ cm} \times 0.1\text{ mm}$ $\text{SA-DTAB-Ca}^{2+}_{100\text{ mM}}$ film, even after being immersed in water for 5 days, still retains a high mechanical strength of about 14 MPa, which can withstand a 1 kg load (Figure 3f). In contrast, both the SA-Ca and SA-DTAB films were broken under this condition (Supplementary Figure 9b).

Conventional petroleum plastics are virtually nondegradable in the natural environment because the long chains with low polarity are difficult to be solvated and interact with microorganisms in nature.^{39,40} In contrast, the polar SA chains, DTA^+ cations, and Ca^{2+} ions endow the film with excellent biodegradation ability. As shown in Figure 4a, the mass of the $\text{SA-DTAB-Ca}^{2+}_{100\text{ mM}}$ plastic decreases continuously with increasing time when the plastic is buried in natural soil. The photograph in Figure 4b shows that the plastic starts to become yellow within 25 days and is broken within 50 days. After 90 days, the broken film can hardly be collected to measure. If the film is subjected to standard soil organism conditions, it takes only 25 days to degrade completely (Figure 4c,d).

Excitingly, the biodegraded $\text{SA-DTAB-Ca}^{2+}_{100\text{ mM}}$ film can enhance soil fertility. The pak choi grown in sand with the buried $\text{SA-DTAB-Ca}^{2+}_{100\text{ mM}}$ film were greener and larger (Figure 4e right) than those grown without the film (Figure 4e left). Quantitative measurements revealed that, after 45 days of growth, both the fresh and dry weights of the pak choi grown in sand with the buried film were 12% higher than those of plants grown without the film (Figure 4f,g). It is noticed that at the 30th day, the fresh weight of the pak choi grown in sand with the film was 40% higher than that grown without the film, indicating that the natural degradation of the SA-DTAB-Ca film generated useful fertilizer for plant growth. It is also noticed that the sand

with the film buried also showed over 30% higher water retention capacity than the sand without film (Figure 4h) in the initial 4 days and over 100% higher water retention in the following fifth to seventh days. These data unambiguously manifest that the SA-DTAB-Ca film promotes plant growth both by enhancing the soil's water retention ability and by increasing the content of fertilizing materials. Since SA is a well-known fertilizer, DTAB is a detergent that can be biodegraded into NH_3 and CO_2 , and Ca^{2+} is bioabsorbable, and this plastic would have no risk of long-term harm to soil.

In summary, we show that the strategy of plastics–fertilizer homology is indeed possible through rationally designed solid-phase molecular self-assembly of biopolysaccharides and surfactants. Since roll-squeezing of the solids has been well-established in industry, it is possible to achieve industrial-scale production of the plastics. When alginate and alkylammonium surfactant were used as the building units followed by calcium coordination, the resultant plastics displayed excellent wet and dry resistance, similar to conventional petroleum plastics, but could be readily degraded in natural soil within 3 months. Meanwhile, the degraded product shows an excellent ability to promote plant growth and water retention of soil, just like a real biomass used to increase the soil fertility. We expect that the strategy of plastics–fertilizer homology would open up a paradigm of natural closed-ring cycles of biodegradable plastics, which is a very promising sustainable choice to tackle the global white pollution. Our next step will extend this strategy to other biomass-sourced polymers to optimize both the mechanical strength and economic cost, making the plastics–fertilizer homology industrially possible.

METHODS

Materials. All chemicals were used as received without further purification. *N,N,N*-Trimethyl-1-dodecanaminium bromide (DTAB) was purchased from Macklin Corporation. Sodium alginate (SA) and calcium chloride (CaCl_2) were purchased from Beijing Tong Guang Fine Chemicals Company. All of the reagents were of AR grade and used as received. The aqueous solutions were prepared by using 18 M Ω Milli-Q water.

Precipitate and Film Formation. To an aqueous solution of DTAB, an aqueous solution of SA was added, reaching final concentrations of 25 mM for the carboxylate negative charges of SA and 25 mM for the ammonium positive charges of DTAB. White precipitates immediately formed after the solutions were mixed, and they were separated from the suspensions by centrifugation with a speed of 5000 rpm. The collected precipitates were then subjected to a pressure imposed by finger pressing, noodle machine manufacturing, or bottle rolling in an ambient environment to get transparent plastic films.

The household noodle machine used was a Baijie Noodle Machine. It is an all-stainless manual household machine for making noodles. For pressing the films, the surfaces of the noodle machine, fingers, and bottles must be washed with deionized water and wiped with a sheet of KIMTECH wipe. A thin sheet of Teflon or a slide was used to separate the precipitate from the finger, bottle, or the surfaces of the noodle machine during pressing. The SA-DTAB-Ca film was fabricated by immersing the SA-DTAB film in CaCl_2 solutions with different concentrations.

Characterization. The weight ratios of C, N, and H were collected from an EL elemental analyzer (Elementar Analysensysteme GmbH). The weight ratios of Ca^{2+} were measured by inductively coupled plasma optical emission spectrometry

(ICP-OES). X-ray diffraction (XRD) measurements were performed using a Rigaku Dmax-2400 diffractometer with Cu K α radiation. The solid samples were placed on clean glass slides for small-angle range tests. The lamellar period d in each sample was calculated using Bragg's law, where $d = \lambda/2 \sin \theta$. The photographs of birefringence were captured by using an LV100N polarizing microscope (Nikon Co.) in an ambient environment at room temperature. Samples were photographed with θ ranging from 0° to 360°, where θ is the angle between the analyzer and the alignment direction of the sample. Fourier transform infrared (FT-IR) spectra were obtained by using a Nicolet Magna-IR 750 spectrophotometer (Thermo Scientific Co.). The method used for SMART iTR was attenuated total reflectance (ATR) with a scanning speed of 2 cm⁻¹. The film and the powder samples were prepared by placing them on clean quartz plates. The UV-vis spectra were recorded on a Shimadzu UV3600plus spectrophotometer equipped with an integrating sphere. Thermogravimetric analysis (TGA) was carried out under a nitrogen flow on a TA Instruments SDT Q600 instrument at a heating rate of 5 °C/min. Middle-angle X-ray scattering (MAXS) measurements were performed using a Ganesha small-angle X-ray scattering system from SAXSLAB Company with Cu K α radiation. The scattering vector q ($q = 4\pi \sin \theta/\lambda$, where θ and λ denote the scattering angle and wavelength of the incident X-ray beam, respectively) and position of the incident X-ray beam on the detector were calibrated using several orders of layer reflections from silver behenate ($d = 58.38$ Å). X-ray photoelectron spectroscopy (XPS) measurements were performed on an AXIS Supra instrument (Kratos Analytical Ltd.) with an X-ray source of Al K α radiation. The mechanical properties of the plastic films were tested by using a WDW3020 electronic universal testing machine at room temperature. Stress-strain data were collected at a strain rate of 5 mm/min. The thicknesses of the films ranged from 20 to 2500 μm . All mechanical tests were conducted on dumbbell-shaped samples.

Soil Fertility Test. To evaluate the ability of the film to promote soil fertility, control experiments with and without the film in sand for plant growth were conducted. Two groups of fine sand with the same weight were put into the same 20 cm \times 20 cm \times 50 cm plastic basin. The 20 cm \times 50 cm plastic was buried in one basin 10 cm below the sand surface. Then 100 cabbage seeds were planted in both basins, watering with 1 L of water for each basin. Three days later, 200 mL of water was sprayed on the sand surfaces of the two groups. Then the two groups of cabbage plants were watered every 3 days with equal amounts of water. From the first week, the same number of cabbage plants (at least five) were removed from each group to measure their weight for comparison, both wet and dried at 80 °C in an oven for 24 h. Three parallel experiments were conducted to ensure the data quality.

Biodegradation. To evaluate the biodegradability, thin films of SA-DTAB-Ca were buried in soil at a depth of 10 cm. The film samples were monitored at a certain time to assess the biodegradation degrees. For the natural biodegradation experiment of SA-DTAB-Ca films, used natural soil was taken from the garden soil of the surrounding residential district in summer (~30 °C, Beijing, 116°20'E, 39°56'N). The obtained soil was used directly without further processing. For the simulated composting biodegradation experiment, the used soil media consisted of the above-mentioned natural soil and commercial microbial powder, uniformly mixed at a dry weight ratio of 4:1. The microbial powder was purchased from WOBIO Bio-

technology Company, mainly composed of microorganisms such as bacillus, yeast, photosynthetic bacteria, lactic acid bacteria, etc.

■ ASSOCIATED CONTENT

SI Supporting Information

The Supporting Information is available free of charge at <https://pubs.acs.org/doi/10.1021/acsmaterialslett.5c00009>.

Supplementary figures and tables: photo of the household noodle machine used for the massive fabrication of SA-DTAB film and the transparency of the resultant film of different thickness; 3D model of DTAB molecule; tensile strength and strain at break of SA-DTAB-Ca_{100 mM} plastic films with different soaking time; tensile strength and strain at break of SA-DTAB-Ca film with different concentration of Ca²⁺ and different soaking time; coordination of Ca²⁺ and SA; schematic of the Ca²⁺-coordination-enhanced hexagonal structure of the SA-DTAB-Ca_{100 mM} plastic film; 2D-MAXS for the SA-DTAB-Ca_{100 mM} plastic films; comparison of mechanical properties between petroleum plastics and SA-DTAB-Ca plastic film; comparison of mechanical properties between SA-DTAB-Ca plastic film and films made of the different combination of the three components; elemental analysis results for the SA-DTAB and SA-DTAB-Ca film (PDF)

■ AUTHOR INFORMATION

Corresponding Authors

Xinxian Ma – Ningxia Key Laboratory of Green Catalytic Materials and Technology, College of Chemistry and Chemical Engineering, Ningxia Normal University, Guyuan 756000, P. R. China; orcid.org/0000-0001-6977-1346; Email: maxinxian@163.com

Yun Yan – Ningxia Key Laboratory of Green Catalytic Materials and Technology, College of Chemistry and Chemical Engineering, Ningxia Normal University, Guyuan 756000, P. R. China; Beijing National Laboratory for Molecular Sciences (BNLMS), College of Chemistry and Molecular Engineering, Peking University, Beijing 100871, China; orcid.org/0000-0001-8759-3918; Email: yunyan@pku.edu.cn

Authors

Jinwan Qi – Ningxia Key Laboratory of Green Catalytic Materials and Technology, College of Chemistry and Chemical Engineering, Ningxia Normal University, Guyuan 756000, P. R. China; Beijing National Laboratory for Molecular Sciences (BNLMS), College of Chemistry and Molecular Engineering, Peking University, Beijing 100871, China

Hongxin Zhao – Beijing National Laboratory for Molecular Sciences (BNLMS), College of Chemistry and Molecular Engineering, Peking University, Beijing 100871, China

Hongjun Jin – Beijing National Laboratory for Molecular Sciences (BNLMS), College of Chemistry and Molecular Engineering, Peking University, Beijing 100871, China; Engineering Research Center of Polymer Green Recycling of Ministry of Education, College of Environmental and Resource Sciences, College of Carbon Neutral Modern Industry, Fujian Normal University, Fuzhou, Fujian 350007, China; orcid.org/0000-0001-8065-6189

Shuitao Gao – Beijing National Laboratory for Molecular Sciences (BNLMS), College of Chemistry and Molecular Engineering, Peking University, Beijing 100871, China
Jianbin Huang – Beijing National Laboratory for Molecular Sciences (BNLMS), College of Chemistry and Molecular Engineering, Peking University, Beijing 100871, China

Complete contact information is available at:

<https://pubs.acs.org/10.1021/acsmaterialslett.5c00009>

Author Contributions

[#]J.Q., H.Z., and H.J. contributed equally.

Notes

The authors declare no competing financial interest.

ACKNOWLEDGMENTS

This work was financially supported by National Natural Science Foundation of China (22332001, 22202006, 22172004). The authors also thanks Dr. Yanxin Sun from the Institute of Microorganism of China for the suggestions on the plant growing experiments in sand.

REFERENCES

- (1) Stegmann, P.; Daioglou, V.; Londo, M.; van Vuuren, D. P.; Junginger, M. Plastic futures and their CO₂ emissions. *Nature* **2022**, *612*, 272–276.
- (2) Kwon, D. Three ways to solve the plastics pollution crisis. *Nature* **2023**, *616*, 234–237.
- (3) Sheng, D.; Jing, S. Y.; He, X. Q.; Klein, A. M.; Kohler, H. R.; Wanger, T. C. Plastic pollution in agricultural landscapes: an overlooked threat to pollination, biocontrol and food security. *Nat. Commun.* **2024**, *15*, 8413.
- (4) Jambeck, J. R.; Geyer, R.; Wilcox, C.; Siegler, T. R.; Perryman, M.; Andrady, A.; Narayan, R.; Law, K. L. Plastic waste inputs from land into the ocean. *Science* **2015**, *347*, 768–771.
- (5) Borrelle, S. B.; Ringma, J.; Law, K. L.; Monnahan, C. C.; Lebreton, L.; McGivern, A.; Murphy, E.; Jambeck, J.; Leonard, G. H.; Hilleary, M. A.; et al. Predicted growth in plastic waste exceeds efforts to mitigate plastic pollution. *Science* **2020**, *369*, 1515–1518.
- (6) Ma, X.; Lin, X. H.; Chang, C. Y.; Duan, B. Chitinous Bioplastic Enabled by Noncovalent Assembly. *ACS Nano* **2024**, *18*, 8906–8918.
- (7) Yu, Y.; Guo, Z.; Zhao, Y.; Kong, K.; Pan, H.; Xu, X.; Tang, R.; Liu, Z. A flexible and degradable hybrid mineral as a plastic substitute. *Adv. Mater.* **2022**, *34*, 2107523.
- (8) Zhou, G. W.; Zhang, H. S.; Su, Z. P.; Zhang, X. Q.; Zhou, H. N.; Yu, L.; Chen, C. J.; Wang, X. A Biodegradable, Waterproof, and Thermally Processable Cellulosic Bioplastic Enabled by Dynamic Covalent Modification. *Adv. Mater.* **2023**, *35*, No. e2301398.
- (9) Xia, Q. Q.; Chen, C. J.; Yao, Y. G.; Li, J. G.; He, S. M.; Zhou, Y. B.; Li, T.; Pan, X. J.; Yao, Y.; Hu, L. B. A strong, biodegradable and recyclable lignocellulosic Bioplastic. *Nat. Sustain.* **2021**, *4*, 627–635.
- (10) Li, Y. X.; Li, S.; Sun, J. Q. Degradable Poly(vinyl alcohol)-Based Supramolecular Plastics with High Mechanical Strength in a Watery Environment. *Adv. Mater.* **2021**, *33*, No. e2007371.
- (11) Fang, X.; Tian, N. G.; Hu, W. Y.; Qing, Y. N.; Wang, H.; Gao, X.; Qin, Y. G.; Sun, J. Q. Dynamically Cross-Linking Soybean Oil and Low-Molecular-Weight Polylactic Acid toward Mechanically Robust, Degradable, and Recyclable Supramolecular Plastics. *Adv. Funct. Mater.* **2022**, *32*, 2208263.
- (12) Guicherd, M.; Khaled, M. B.; Alvarez, P.; Kamionka, E.; Gavalda, S.; Cioci, G.; Tournier, V.; Guéroult, M.; Noël, M.; Nomme, J.; et al. An engineered enzyme embedded into PLA to make self-biodegradable plastic. *Nature* **2024**, *631*, 884–890.
- (13) Tournier, V.; Topham, C. M.; Gilles, A.; David, B.; Folgoas, C.; Moya-Leclair, E.; Kamionka, E.; Desrousseaux, M. L.; Texier, H.; Gavalda, S.; et al. An engineered PET depolymerase to break down and recycle plastic bottles. *Nature* **2020**, *580*, 216–219.
- (14) Thompson, R. C.; Courtene-Jones, W.; Boucher, J.; Pahl, S.; Raubenheimer, K.; Koelmans, A. A. Twenty years of microplastics pollution research—what have we learned? *Science* **2024**, *386*, eadl2746.
- (15) MacLeod, M.; Arp, H. P. H.; Tekman, M. B.; Jahnke, A. The global threat from plastic pollution. *Science* **2021**, *373*, 61–65.
- (16) Kane, I. A.; Clare, M. A.; Miramontes, E.; Wogelius, R.; Rothwell, J. J.; Garreau, P.; Pohl, F. Seafloor microplastic hotspots controlled by deep-sea circulation. *Science* **2020**, *368*, 1140–1145.
- (17) Shieh, P.; Zhang, W.; Husted, K. E. L.; Kristufek, S. L.; Xiong, B.; Lundberg, D. J.; Lem, J.; Veysset, D.; Sun, Y.; Nelson, K. A.; et al. Cleavable comonomers enable degradable, recyclable thermoset plastics. *Nature* **2020**, *583*, 542–547.
- (18) Haussler, M.; Eck, M.; Rothauer, D.; Mecking, S. Closed-loop recycling of polyethylene-like materials. *Nature* **2021**, *590*, 423–427.
- (19) Christensen, P. R.; Scheuermann, A. M.; Loeffler, K. E.; Helms, B. A. Closed-loop recycling of plastics enabled by dynamic covalent diketoenamine bonds. *Nat. Chem.* **2019**, *11*, 442–448.
- (20) Lu, X. Y.; Xie, P.; Li, X.; Li, T. Q.; Sun, J. Q. Acid-Cleavable Aromatic Polymers for the Fabrication of Closed-Loop Recyclable Plastics with High Mechanical Strength and Excellent Chemical Resistance. *Angew. Chem., Int. Ed.* **2024**, *63*, No. e202316453.
- (21) Zhang, Z. Q.; Lei, D.; Zhang, C. X.; Wang, Z. Y.; Jin, Y. H.; Zhang, W.; Liu, X. K.; Sun, J. Q. Strong and Tough Supramolecular Covalent Adaptable Networks with Room-Temperature Closed-Loop Recyclability. *Adv. Mater.* **2023**, *35*, No. e2208619.
- (22) Serrano, D.; Aguado, J.; Escola, J. Developing advanced catalysts for the conversion of polyolefinic waste plastics into fuels and chemicals. *ACS Catal.* **2012**, *2*, 1924–1941.
- (23) Jing, Y.; Wang, Y.; Furukawa, S.; Xia, J.; Sun, C.; Hülsley, M. J.; Wang, H.; Guo, Y.; Liu, X.; Yan, N. Towards the Circular Economy: Converting Aromatic Plastic Waste Back to Arenes over a Ru/Nb₂O₅ Catalyst. *Angew. Chem., Int. Ed.* **2021**, *60*, 5527–5535.
- (24) Ronkvist, Å. M.; Xie, W.; Lu, W.; Gross, R. A. Cutinase-catalyzed hydrolysis of poly (ethylene terephthalate). *Macromolecules* **2009**, *42*, 5128–5138.
- (25) Geyer, R.; Jambeck, J. R.; Law, K. L. Production, use, and fate of all plastics ever made. *Sci. Adv.* **2017**, *3*, No. e1700782.
- (26) Chamas, A.; Moon, H.; Zheng, J. J.; Qiu, Y.; Tabassum, T.; Jang, J. H.; Abu-Omar, M.; Scott, S. L.; Suh, S. Degradation Rates of Plastics in the Environment. *ACS Sustain. Chem. Eng.* **2020**, *8*, 3494–3511.
- (27) Hillmyer, M. A. The promise of plastics from plants. *Science* **2017**, *358*, 868–870.
- (28) Gross, R. A.; Kalra, B. Biodegradable Polymers for the Environment. *Science* **2002**, *297*, 803–807.
- (29) Cywar, R. M.; Rorrer, N. A.; Hoyt, C. B.; Beckham, G. T.; Chen, E. Y. X. Bio-based polymers with performance-advantaged properties. *Nat. Rev. Mater.* **2022**, *7*, 83–103.
- (30) Merino, D.; Salcedo, M. F.; Mansilla, A. Y.; Casalougué, C. A.; Alvarez, V. A. Development of Sprayable Sodium Alginate-Seaweed Agricultural Mulches with Nutritional Benefits for Substrates and Plants. *Waste Biomass Valor.* **2021**, *12*, 6035–6043.
- (31) Immirzi, B.; Santagata, G.; Vox, G.; Schettini, E. Preparation, characterisation and field-testing of a biodegradable sodium alginate-based spray mulch. *Biosyst. Eng.* **2009**, *102*, 461–472.
- (32) Xie, M. Q.; Che, Y. X.; Liu, K.; Jiang, L. X.; Xu, L. M.; Xue, R. R.; Drechsler, M.; Huang, J. B.; Tang, B. Z.; Yan, Y. Caking-Inspired Cold Sintering of Plastic Supramolecular Films as Multifunctional Platforms. *Adv. Funct. Mater.* **2018**, *28*, 1803370.
- (33) Jin, H. J.; Xie, M. Q.; Wang, W. K.; Jiang, L. X.; Chang, W. Y.; Sun, Y.; Xu, L. M.; Zang, S. H.; Huang, J. B.; Yan, Y.; et al. Pressing-Induced Caking: A General Strategy to Scale-Span Molecular Self-Assembly. *CCS Chem.* **2020**, *2*, 98–106.
- (34) Jin, H. J.; Ma, C.; Wang, W. K.; Cai, Y. T.; Qi, J. W.; Wu, T. Y.; Liao, P. L.; Li, H. P.; Zeng, Q.; Xie, M. Q.; et al. Using Molecules with Superior Water-Plasticity to Build Solid-Phase Molecular Self-Assembly: Room-Temperature Engineering Mendable and Recyclable Functional Supramolecular Plastics. *ACS Mater. Lett.* **2022**, *4*, 145–152.

(35) Qi, J. W.; Wu, T. Y.; Wang, W. K.; Jin, H. J.; Gao, S. T.; Jiang, S. S.; Huang, J. B.; Yan, Y. Solid-phase molecular self-assembly facilitated supramolecular films with alternative hydrophobic/hydrophilic domains for skin moisture detection. *Aggregate* **2022**, *3*, No. e173.

(36) Jin, H.; Lin, W.; Wu, Z.; Cheng, X.; Chen, X.; Fan, Y.; Xiao, W.; Huang, J.; Qian, Q.; Chen, Q.; Yan, Y. Surface Hydrophobization Provides Hygroscopic Supramolecular Plastics Based on Polysaccharides with Damage-Specific Healability and Room-Temperature Recyclability. *Adv. Mater.* **2023**, *35*, e2207688.

(37) Jordan, J. L.; Casem, D. T.; Bradley, J. M.; Dwivedi, A. K.; Brown, E. N.; Jordan, C. W. Mechanical Properties of Low Density Polyethylene. *J. dynamic behavior mater.* **2016**, *2*, 411–420.

(38) Ciccio, N. R.; Shi, J. X.; Pal, S.; Hua, M.; Malollari, K. G.; Lizandara-Pueyo, C.; Risto, E.; Ernst, M.; Helms, B. A.; Messersmith, P. B.; Hartwig, J. F. Diverse functional polyethylenes by catalytic amination. *Science* **2023**, *381*, 1433–1440.

(39) Kim, M. S.; Chang, H.; Zheng, L.; Yan, Q.; Pflieger, B. F.; Klier, J.; Nelson, K.; Majumder, E. L. W.; Huber, G. W. A Review of Biodegradable Plastics: Chemistry, Applications, Properties, and Future Research Needs. *Chem. Rev.* **2023**, *123*, 9915–9939.

(40) Taghavi, N.; Udugama, I. A.; Zhuang, W. Q.; Baroutian, S. Challenges in biodegradation of non-degradable thermoplastic waste: From environmental impact to operational readiness. *Biotechnol. Adv.* **2021**, *49*, 107731.